CHAPTER 8

BURSTING IN COUPLED CELL SYSTEMS

Martin Golubitsky
Krešimir Josić
Department of Mathematics, University of Houston
Houston TX 77204-3008, USA
e-mail: mg@uh.edu; josic@math.uh.edu

LieJune Shiau
Department of Mathematics, University of Houston–Clear Lake
Houston TX 77058, USA
e-mail: shiau@cl.uh.edu

Periodic bursting in fast-slow systems can be viewed as closed paths through the unfolding parameters of degenerate singularities. Using this approach we show that bursting in coupled systems can have interesting behavior. We focus on two identical cell systems and use the $\mathbf{Z}_2$ symmetry present in such systems to illustrate interesting bursting phenomena. In particular, we show that Hopf/Hopf mode interactions can lead to bursting between in phase and out of phase periodic solutions and symmetry-breaking Takens-Bogdanov singularities can lead to bursting that randomly chooses between two (symmetrically related) limit cycles.

8.1. Introduction

Many processes in nature are characterized by transitions between different modes of activity, such as periodic, quasiperiodic, chaotic and quiescent states. An example of an autonomous differential equation whose behavior alternates between near steady-states and trains of approximate spike-like oscillations was analyzed by Rinzel [13, 16], and such behavior has since been referred to as bursting. From a mathematical point of view, it is also natural to consider transitions between other attracting states in a similar

vein, and this is the viewpoint we will adopt in this chapter.

The large number of possible states and transitions between them necessitates a coherent method of classifying different types of bursting systems. Early classifications using roman numerals assigned to the different bursters in the order of their description in the literature, or based on qualitative properties of the timeseries proved impractical. Systematic methods were soon introduced (see [2, 11], for example).

In [6, 11] a method was introduced for classifying the types of bursting that occur in models in which variables evolve on two different timescales, i.e., fast-slow systems. The classification is based on the observation that the bifurcations of the fast system that lead to bursting can be collapsed to a single local bifurcation, generally of higher codimension. The bursting is recovered as the slow variables periodically trace a closed path in the universal unfolding of this singularity. The codimension of a periodic bursting type is then defined to be the codimension of the singularity in whose unfolding it first appears. Using this definition, all of the known universal unfoldings of codimension one and two bifurcations were analyzed to classify the codimension one and two bursters.

This local approach has several advantages over global analytic and geometric methods that are also used to classify bursters. Many bifurcations that are first observed globally can be studied more easily by using the unfolding theory of degenerate singularities, since the local theory provides methods by which global phenomena can be found locally using calculus and numerical techniques. Moreover, the local theory provides a rational method of classification by codimension that indicates how complex a system needs to be in order for it to support bursters of given types.

The goal of this chapter is to illustrate how the ideas described in [6] can be extended to networks of bursting systems. To avoid technicalities, and give an accessible introduction to these ideas, we only consider networks of two coupled identical cells. The assumption that the cells are identical leads to $\mathbf{Z}_2$ symmetry in the equations of motions. The unfoldings of singularities in the presence of such symmetries can be very different from the general case and lead to new and surprising phenomena.

The chapter is organized as follows. In section 8.2, we review the theory introduced in [6], and in section 8.3 we adapt the discussion to two-cell systems. In section 8.4 we review the codimension one and two bifurcations in $\mathbf{Z}_2$-equivariant systems. Bursters associated to steady-state pitchfork bifurcations are discussed in section 8.5. Those associated with Hopf/Hopf mode interactions and Takens-Bogdanov bifurcations are discussed in sections 8.6

and 8.7. Hopf/Hopf mode interactions can lead to bursting between in phase and out of phase periodic solutions and symmetry-breaking Takens-Bogdanov bifurcations can lead to a form of chaotic dynamics where the bursting randomly chooses between two symmetrically related limit cycles and steady-states. A similar phenomenon can occur in pitchfork bifurcations, but only when noise is added to the system.

8.2. Unfolding Theory and Bursting in Fast-Slow Systems

We consider bursting that occurs in models consisting of variables that evolve on a fast and a slow timescale, and can therefore be described by equations of the form

$$\begin{aligned} x' &= f(x, y) \\ y' &= \varepsilon g(x, y), \end{aligned}$$

where $\varepsilon > 0$ is small, $x \in \mathbf{R}^n$, $y \in \mathbf{R}^k$, $f : \mathbf{R}^n \times \mathbf{R}^k \to \mathbf{R}^n$, and $g : \mathbf{R}^n \times \mathbf{R}^k \to \mathbf{R}^k$.

In periodic bursters, the slow variables y oscillate periodically, and thus provide a time-periodic forcing in the fast x' equation. In turn, the solution of the fast equation visits various invariant sets in order. The slow variables either provide this forcing effectively *without* feedback from the fast system, or *with* feedback from the fast system. In the former case, the system may be modeled as:

$$\begin{aligned} x' &= f(x, y) \\ y' &= \varepsilon g(y), \end{aligned} \tag{2}$$

with the slow component only depending on the slow variable y. A reduction to (2) can also be made in the latter case, under certain assumptions.

Assuming that the slow system varies periodically, we rewrite (2) as

$$x' = f(x, y(\varepsilon t)). \tag{3}$$

If ε is sufficiently small, the solution of (3) visits the stable invariant states of the frozen system

$$x' = f(x, y^*)$$

where $y^* = y(\varepsilon t^*)$ for some t^*, i.e., the time-periodic evolution of $y(\varepsilon t)$ forces the solution trajectory $x(t)$ to transition between these invariant sets. The transition from one invariant state to another occurs at values of y^* at which the state that is currently shadowed by the orbit of the fast system, loses stability in some type of bifurcation. As $y(\varepsilon t)$ passes such a

value, the orbit of (3) leaves the vicinity of such a state and is attracted to another state which is stable for the current value of the "parameter" y. We note that for analytic systems the orbit may remain in the vicinity of an unstable state long after $y(\varepsilon t)$ passes through a bifurcation value for the frozen system. This *delayed loss of stability* is discussed in more detail in [10, 14], and references therein. Although this phenomenon does not typically persist for noisy systems, it can be observed in numerical simulations, as is demonstrated below.

A *periodic burster type* is determined by the set of stable attractors (equilibria, periodic orbits, *etc.*) that the system visits, as well as the bifurcations in which these states lose their stability. For a precise definition see [6].

To illustrate the local birth of periodic bursters, we assume that the frozen system

$$x' = f(x, 0)$$

has a singularity of codimension k at $x = 0$ and that the y variables are universal unfolding parameters for this singularity. In this context, we assume that the unfolding theorem is valid and $y(\varepsilon t)$ is a small amplitude periodic path in $\mathbf{R}^k$. Of course, our discussion only refers to an unspecified neighborhood of the origin in $\mathbf{R}^k$, so that the convention of writing the parameter space of k parameters as $\mathbf{R}^k$ is a slight abuse of notation.

Locally, near the origin, the universal unfolding defines a codimension one transition variety $\mathcal{V} \subset \mathbf{R}^k$. This variety consists of parameter values at which singularities of codimension at least one occur. These singularities include, but are not limited to, saddle-node bifurcations, Hopf bifurcations, and homoclinic trajectories.

For different values on the periodic orbit $y(\varepsilon t)$, different states may be stable, and may lose their stability as the path crosses $\mathcal{V}$. Therefore traversing a path in the unfolding of this singularity can lead to transitions between various stable states, and hence periodic bursting. Note that many different paths can lead to the same type of transitions, and can be considered *path equivalent* (for a precise definition see [6]). In fact, typically a small change in the path will preserve the bursting type observed in the fast system.

Among all of those singularities whose unfoldings contain a given bursting type, the one with smallest codimension gives an intrinsic measure of the complexity of that burster. The *codimension* of a periodic bursting type is the minimum codimension of a bifurcation point in the fast system in whose unfoldings that type of bursting occurs.

In [6] codimension one bursters (from a nondegenerate Hopf bifurcation in the fast subsystem), codimension two bursters (from the cusp singularity, degenerate Hopf bifurcation, Takens-Bogdanov bifurcation, Hopf-steady state mode interaction, and Hopf-Hopf mode interaction), and certain codimension three bursters are described from this viewpoint. Somewhat surprisingly, the systems traditionally labeled as Type III (or elliptic) bursters have codimension two, whereas the other most commonly studied bursters — those labeled as Types Ia (square-wave), Ib, II (parabolic) and IV — first occur in the unfoldings of a codimension three bifurcation [2].

The path in the unfolding of the degenerate Hopf bifurcation that leads to Type III bursting, and a typical resulting timeseries is shown in Fig. 8.1. The path through the unfolding of this codimension two bifurcation is depicted on the lower left. Suppose we start at the leftmost point on the path. For this value of the slow parameter the fast system approaches a stable fixed point at the origin. As the slow system traverses the path, this fixed point loses stability in a subcritical Hopf bifurcation, and, after a delay, the orbit of the fast system approaches the unique periodic orbit that exists in this region of parameter space. As the slow system follows the path through the unfolding from right to left, this periodic orbit loses stability in a collision with an unstable periodic orbit (the same orbit that arose in the subcritical Hopf bifurcation discussed earlier). After this bifurcation, the fast system again approaches the stable fixed point at the origin, and the process repeats.

8.3. Bursting in Two Coupled Cells

In many applications one studies the dynamics of two identical coupled cells. We further assume that each cell is a fast-slow system, and that the cells are coupled symmetrically, so that the evolution of the network is described by

$$\begin{aligned} x_1' &= f(x_1, y_1, x_2, y_2) & \qquad x_2' &= f(x_2, y_2, x_1, y_1) \\ y_1' &= \varepsilon g(x_1, y_1, x_2, y_2) & \qquad y_2' &= \varepsilon g(x_2, y_2, x_1, y_1). \end{aligned}$$

It is frequently observed in practice that the slow variables of such a system can be (approximately) synchronous, even when the fast variables are desynchronized. Suppose that each cell bursts, and that the active state is oscillatory. Moreover, assume that the average of the fast, oscillating variables x_1 and x_2 is equal, although the two are not necessarily synchronized. In this case, after averaging the fast variables over each cycle in their

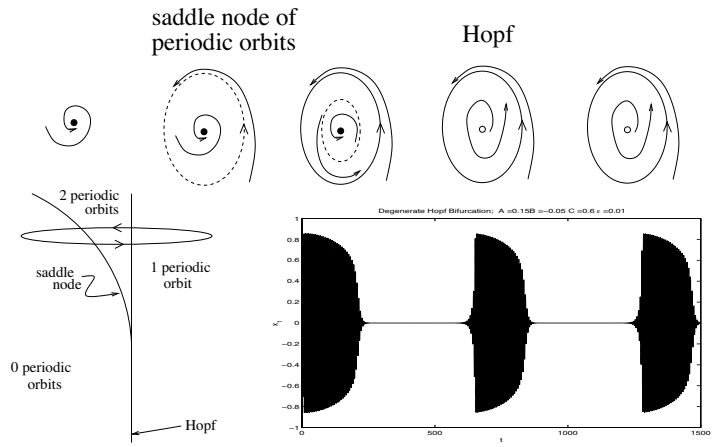

Fig. 8.1. A schematic representation of Type III elliptic bursting. The stable and unstable periodic orbits collide in a saddle-node of periodic orbits, causing the system to return to the quiescent state. The slow passage effect is manifested at the beginning of each active phase.

oscillations, we obtain the following equations for the slow variables

$$y_1' = \varepsilon g(\bar{x}, y_1, \bar{x}, y_2) \qquad y_2' = \varepsilon g(\bar{x}, y_2, \bar{x}, y_1).$$

The manifold $\Sigma_y = \{(y_1, y_2) : y_1 = y_2\}$ is invariant for this reduced system. Therefore, under these conditions, the slow variables can be expected to behave synchronously, even when the fast variables do not.

Alternatively, consider a coupled system depending on an ambient parameter which slowly changes (for instance an extracellular concentration of calcium which changes slowly compared to the internal dynamics of the two cells). Let us assume that the network consists of two identical, symmetrically coupled cells which depend in the same way on the ambient parameter.

In both of these cases it is reasonable to look at the following model

$$x_1' = f(x_1, x_2, p(\varepsilon t)) \qquad x_2' = f(x_2, x_1, p(\varepsilon t)). \tag{8}$$

In the first example, $p(\varepsilon t)$ corresponds to the synchronous slow variables. In the second it represents the slowly varying parameter. In many situations $p(\varepsilon t)$ is periodic in time. This occurs for many systems modeling bursting behavior. This is the type of model we will analyze.

Note that the diagonal $\Sigma_x = \{(x_1, x_2) : x_1 = x_2\}$ =Fix($\mathbf{Z}_2$) is an invariant submanifold for system (8) and contains the synchronous solutions of the system. We will concentrate on bifurcations from synchronous solutions, that is from different orbits contained in Σ_x.

We take the approach outlined in the previous section and developed in [6], and consider periodic paths through the unfolding of low codimension bifurcations. Since (8) is $\mathbf{Z}_2$-equivariant, this will be reflected in the unfoldings that we consider.

8.4. $\mathbf{Z}_2$-Equivariant Bifurcations

In this section we review the codmension one and codimension two $\mathbf{Z}_2$-equivariant local bifurcations from a $\mathbf{Z}_2$-invariant equilibrium x_0 of a system of differential equations $\dot{x} = h(x)$ where $x \in \mathbf{R}^n$.

There are four types of codimension one $\mathbf{Z}_2$-equivariant bifurcations: two steady-state and two Hopf bifurcations. These bifurcations are summarized in Table 8.1. Let γ be the nonidentity symmetry in $\mathbf{Z}_2$. Let $J = (dh)_{x_0}$ be the Jacobian matrix of the ODE system at x_0. It follows from the chain rule that $J\gamma = \gamma J$, and hence that

$$\mathbf{R}^n = \Sigma \oplus \Sigma^{\perp}$$

where Σ and $\Sigma^{\perp}$ are J-invariant, γ acts trivially on Σ and as $-I$ on $\Sigma^{\perp}$. More explicitly,

$$\Sigma = \{(x_1, x_1) : x_1 \in \mathbf{R}^k\} \quad \text{and} \quad \Sigma^{\perp} = \{(x_1, -x_1) : x_1 \in \mathbf{R}^k\}$$

Table 1: Codimension one $\mathbf{Z}_2$-equivariant bifurcations

Bifurcation	Type	Solution Type
steady-state	Σ	saddle-node of $\mathbf{Z}_2$-invariant states
steady-state	$\Sigma^{\perp}$	pitchfork to symmetry related pairs
Hopf	Σ	$\mathbf{Z}_2$-invariant periodic solutions
Hopf	$\Sigma^{\perp}$	half-period out of phase periodic solutions

Generically, the eigenspaces of J are contained either in Σ or $\Sigma^{\perp}$. The two steady-state bifurcations correspond to a simple zero eigenvalue with eigenvector in Σ or in $\Sigma^{\perp}$. Generically, the first case leads to a saddle node bifurcation of γ-invariant equilibria (that is, the steady states lie inside Fix(γ) = Σ). Generically, the second case leads to a pitchfork bifurcation

(that is, to pairs of γ related equilibria bifurcating from a branch of γ-invariant equilibria).

The two Hopf bifurcations correspond to simple purely imaginary eigenvalues with two-dimensional critical subspace W in Σ or in $\Sigma^\perp$. Each of these bifurcations leads generically to a unique branch of periodic solutions from a branch of γ-invariant equilibria. In the first case the periodic solutions themselves are γ-invariant (that is, lie inside $\mathrm{Fix}(\gamma)$). In the second case, the periodic solutions $x(t)$ are half-period out of phase periodic solutions (that is, $\gamma x(t) = x(t + T/2)$ where T is the period of $x(t)$).

Codimension two bifurcations appear in two types: mode interactions and nonlinear degeneracies. In this paper we consider three types of mode interaction: steady-state/steady-state, steady-state/Hopf, and Hopf/Hopf. Each of these three types appear in three different ways: Σ-Σ, Σ-$\Sigma^\perp$, and $\Sigma^\perp$-$\Sigma^\perp$ mode interactions. So there are nine different mode interactions that can be considered. Note that generically the steady-state/steady-state mode interactions Σ-Σ and $\Sigma^\perp$-$\Sigma^\perp$ occur as Takens-Bogdanov codimension two bifurcations. We will not present detailed results from all nine of these different mode interactions. For the most part, the analyses of these codimension two bifurcations may be found in the literature or are simple adaptations of what is in the literature. See [8].

We end this section by commenting on what is needed for these various bifurcations to occur in a coupled cell system

$$\begin{aligned} \dot{x}_1 &= f(x_1, x_2) = \alpha x_1 + \beta x_2 + \cdots \\ \dot{x}_2 &= f(x_2, x_1) = \alpha x_2 + \beta x_1 + \cdots \end{aligned}$$

where $x_1, x_2 \in \mathbf{R}^k$, α and β are $k \times k$ matrices, and the assumed equilibrium is at $x_0 = (0, 0)$. Here α is the linearized internal dynamics and β is the linearized coupling. Moreover

$$J|\Sigma = \alpha + \beta \quad \text{and} \quad J|\Sigma^\perp = \alpha - \beta$$

Thus, a steady-state Σ bifurcation occurs when $\alpha + \beta$ has a zero eigenvalue, etc. In general, we will only consider bifurcations and mode interactions when the dimension k of each cell is minimum. For example, we take $k = 1$ for steady-state bifurcations and $k = 2$ for Hopf bifurcations. Note that we can assume $k = 2$ for Σ-Σ and $\Sigma^\perp$-$\Sigma^\perp$ Takens-Bogdanov singularities but we can take $k = 1$ for Σ-$\Sigma^\perp$ steady-state/steady-state mode interactions.

8.5. Pitchfork Bifurcation

Consider a system of the form (8) in which the two cells have one-dimensional internal dynamics. As discusses in section 8.3, if the system has a fixed point in Σ, two types of steady-state bifurcations will be typical, a bifurcation inside the synchrony subspace Σ which will generically be a saddle-node bifurcation, and a bifurcation in the direction normal to Σ which will typically be a pitchfork bifurcation.

The truncated normal form of the pitchfork bifurcation is given by

$$\xi' = \xi(p \pm \xi^2). \tag{13}$$

This bifurcation will occur in a direction tangent to the space $\Sigma^\perp$, and therefore we can think of ξ as a coordinate along the center manifold in which this bifurcation occurs. To examine the bifurcations it is therefore natural to write the normal form in the coordinates

$$\xi = \frac{x_1 - x_2}{2} \qquad \eta = \frac{x_1 + x_2}{2} \tag{14}$$

Note that η is the coordinate along the linear submanifold Σ corresponding to the synchronized state. The subspace $\Sigma^\perp$ must be stable for the bifurcation to be observable; therefore we assume that equation for η is

$$\eta' = -\lambda\eta \qquad\qquad \lambda > 0. \tag{15}$$

We can use (14) to rewrite the pitchfork bifurcation in the original network coordinates as[a]

$$\begin{aligned} x_1' &= (x_1 - x_2)\left(p - (\tfrac{x_1-x_2}{2})^2\right) - \lambda(x_1 + x_2) \\ x_2' &= -(x_1 - x_2)\left(p - (\tfrac{x_1-x_2}{2})^2\right) - \lambda(x_1 + x_2). \end{aligned} \tag{16}$$

As discussed in the introduction, we can observe bursting behavior if we let the bifurcation parameter vary slowly, and move through the bifurcation point $p = 0$. In particular, let

$$p = p(\varepsilon t) = C\sin(\varepsilon t) + A. \tag{17}$$

The state $x_1 = x_2$ becomes unstable as p becomes positive. Due to delayed passage [12], the system does not follow the branch of equilibria that would be obtained in the quasi-steady-state approximation. See Fig. 8.2.

Note that the manifold Σ is invariant for the system (16)-(17). Since this is a codimension one manifold in the phase space of the system, either x_1

[a]In writing equations (16), as well as equations (20), and (25), we omit certain constants that multiply the right hand side. This change corresponds to a reparametrization of time, and does not affect the solutions in any other way.

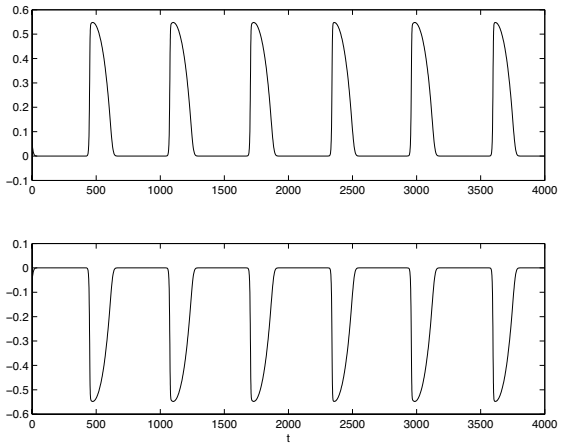

Fig. 8.2. The time series for x_1 (top) and x_2 (bottom) are half period out of phase in(16) with $p(\varepsilon t) = 0.4\sin(\varepsilon t) - 0.1$ and $\varepsilon = 0.001$.

will increase, and x_2 will decrease during the burst, if the initial conditions satisfy $x_1(0) - x_2(0) > 0$ (this is the situation in Fig. 8.2). If $x_2(0) - x_1(0) > 0$, the orbit is attracted to the symmetrical attractor, and x_1 and x_2 switch places.

If we look at the orbit in the (ξ, η, p) coordinates, then ξ is contracted exponentially to $\xi = 0$ when $p < 0$, that is before the onset of the pitchfork bifurcation. Since p evolves on a much longer timescale than ξ an exponentially small amount of noise can kick ξ across the manifold $\{\xi = 0\}$, which corresponds to the manifold Σ in the (x_1, x_2, p) coordinates.

Therefore in the cell coordinates, a small amount of noise will allow the trajectory to cross the synchronized state Σ. If the noise is small, the deterministic dynamics will eventually force the system into a burst. If the noise intensity is equal in both cells, the system will be equally likely to burst in the positive or negative ξ direction. As a result, the system will be equally likely to burst in either of the two modes. This is illustrated in Fig. 8.3. To create the figure we have added a small perturbation of the form $\delta\sin(t)$, with $\delta \ll 1$ to equation (13). Since the frequency of this perturbation is much higher than the frequency of p in (17), this term

effectively acts like noise. For details on the slow passage through a pitchfork bifurcation in the presence of noise, we refer the reader to [1, 4].

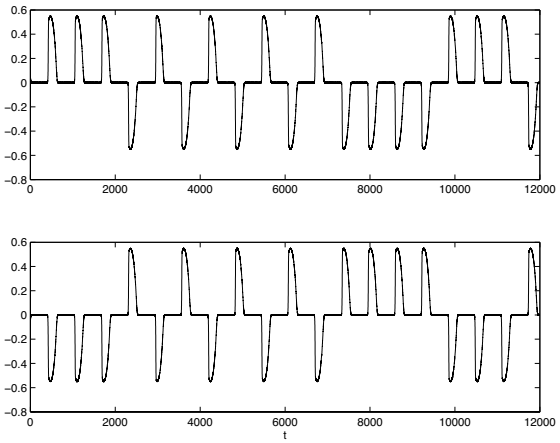

Fig. 8.3. The time series for x_1 (top) and x_2 (bottom) are half period out of phase, and randomly switch branches as noise $(0.01\sin(\pi t))$ is added to the pitchfork bifurcation (16); $p(\varepsilon t) = 0.4\sin(\varepsilon t) - 0.1$ and $\varepsilon = 0.001$.

8.6. Hopf / Hopf Mode Interactions

In this section we consider different phenomena that are possible when the network undergoes Hopf bifurcations. Harkin *et al.* [9] show that two bubbles in a fluid that descend under gravity can transition between in phase and out of phase oscillation. This observation motivates our discussion of bursting arising from Hopf / Hopf mode interactions. We suppose that two Hopf modes, one preserving $\mathbf{Z}_2$-symmetry and one breaking that symmetry, bifurcate simultaneously from a $\mathbf{Z}_2$-invariant equilibrium and show that bursting between in phase and out of phase oscillation can occur robustly in the unfoldings of this mode interaction.

We assume that the frequencies of the two modes are irrationally related. It follows that the Poincaré-Birkhoff normal form of the center manifold vector fields decouple into phase-amplitude equations [8] and that the

amplitude equations have $\mathbf{Z}_2 \oplus \mathbf{Z}_2$-symmetry. We use the results in chapter X of [7] to describe the unfoldings of this mode interaction. The universal unfolding in the vicinity of a Hopf bifurcation of this mode interaction is given by

$$\begin{aligned} \xi' &= -i\xi - (|\xi|^2 + m|\eta|^2 - p)\xi \\ \eta' &= -\sqrt{2}\, i\eta - (n|\xi|^2 + |\eta|^2 - (p-\sigma))\eta \end{aligned} \tag{18}$$

where $\xi, \eta \in \mathbf{C}$, and p is the bifurcation parameter. The frequency of oscillation in the second equation is multiplied by $\sqrt{2}$ to avoid resonances. The equations are given in complex coordinates, and we can use $\xi = \xi_r + i\xi_i$ and $\eta = \eta_r + i\eta_i$ to transform the equations to the real coordinates $(\xi_r, \xi_i, \eta_r, \eta_i) \in \mathbf{R}^4$. The values of m and n determine several possible bifurcation scenarios. The parameter σ determines the location of a secondary Hopf bifurcation (see Fig. 8.4 and [7]).

To obtain the normal form of the $\mathbf{Z}_2$ equivariant Hopf bifurcations in the network coordinates we again think of ξ as a coordinate transversal to the synchronization manifold, and η as a coordinate along to the synchronization manifold. Therefore

$$\xi = \frac{z_1 - z_2}{2} \qquad \eta = \frac{z_1 + z_2}{2} \tag{19}$$

can be used to transform equation (18) into the network coordinates. In the new coordinates we have

$$\begin{aligned} z_1' = &-z_1\left[(2+m+n)\rho + (m-n)\tau - 4(2p-\sigma) + 4(\sqrt{2}+1)i\right] \\ &-z_2\left[(n-m)\rho + (2-m-n)\tau + 4\sigma + 4(\sqrt{2}-1)i\right], \\ z_2' = &-z_1\left[(n-m)\rho + (2-m-n)\tau + 4\sigma + 4(\sqrt{2}-1)i\right] \\ &-z_2\left[(2+m+n)\rho + (m-n)\tau - 4(2p-\sigma) + 4(\sqrt{2}+1)i\right]. \end{aligned} \tag{20}$$

where $\rho = |z_1|^2 + |z_2|^2$ and $\tau = z_1\bar{z}_2 + \bar{z}_1 z_2$.

In the following we let $m = 4$, $n = 1/2$, and $\sigma = 1/4$, which corresponds to case 2 on p. 434 of [7]. When $p < 0$ the origin is a globally attracting fixed point. The origin loses stability at $p = 0$ in a Hopf bifurcation which gives rise to a stable state in which the two systems are half period out of phase. This state remains stable in some interval $p > 0$, and loses stability in a subcritical Neimark-Sacker bifurcation at $p = p_{\mathrm{NS}}^2$.

Note that there is a Hopf bifurcation at the origin when $p = \sigma$ giving rise to an initially unstable periodic solution which lies inside

$$\Sigma = \{(z_1, z_2) \in \mathbf{C}^2 : z_1 = z_2\} = \{(\xi, \eta) \in \mathbf{C}^2 : \xi = 0\}\}$$

and therefore corresponds to the synchronous state. The unstable torus that is born at the Neimark-Sacker bifurcation at p_{NS}^2 collides with this

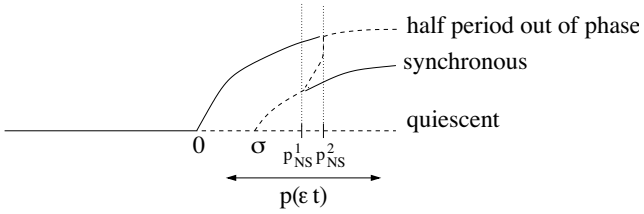

Fig. 8.4. Bifurcation diagram corresponding to equation (18). The solid and dashed lines represent stable and unstable states. The ξ state is synchronous and the η state is asynchronous.

synchronous state in a reverse Neimark-Sacker bifurcation at $p^1_{\rm NS}$in which the synchronous state becomes stable.

We again assume that the bifurcation parameter p varies slowly in time. For the parameter values given above we let $p(\varepsilon t) = 0.3\sin(\varepsilon t) + 0.4$ and $\varepsilon = 0.005$ which corresponds to the path shown in Fig. 8.4.

As the parameter sweeps the diagram from left to right, the state in which the oscillators are half period out of phase loses stability at $p = p^2_{\rm NS}$, and the system is attracted to the synchronous state. As the parameter evolves in the opposite direction, the synchronous state in turn loses stability at $p = p^1_{\rm NS}$, and the system jumps back to the out of phase state. Therefore the system is observed to burst between an *in-phase* and an *out-of-phase* state (see Fig. 8.5).

Note that during the time $\eta \neq 0$, the variable ξ decays to 0 exponentially. Since the manifold Σ is invariant, orbits that come within numerical accuracy of the manifold will never leave it in a numerical simulation. To avoid such problems, as well as reduce the slow passage effects, we added a small sinusoidal term with frequency $\mathcal{O}(1)$ to the equations (20). The exact form of the term is not of importance.

8.7. Takens-Bogdanov Bifurcation with $\mathbf{Z_2}$ Symmetry

Consider the two-coupled cell system

$$x_1' = f(x_1, x_2, p_1, p_2)$$
$$x_2' = f(x_2, x_1, p_1, p_2)$$

in which the two cells both have two-dimensional internal dynamics. We again consider systems which have equilibria on the diagonal Σ which are

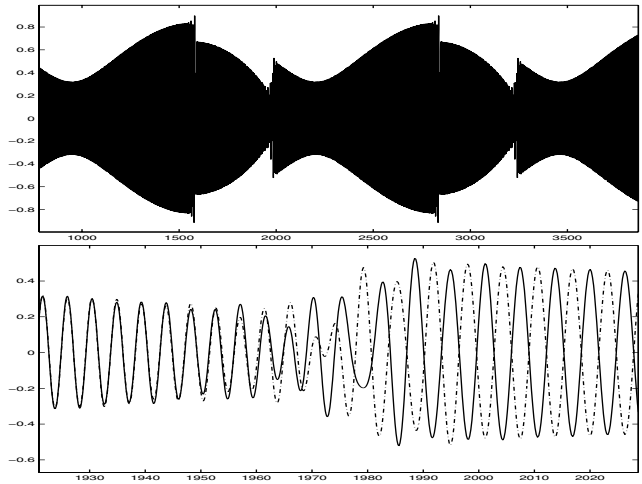

Fig. 8.5. Bursting corresponding to the path shown in Fig. 8.4. The timeseries of Re z_1 (solid line) and Re z_2 (dashed line) are shown in both figures. A portion of the top figure is enlarged in the bottom figure to illustrate the transition between the synchronous and the half period out of phase state.

close to a bifurcation. Without loss of generality, we assume the equilibrium is at the origin.

As in the case of the pitchfork bifurcation, we restrict our attention to bifurcations that break $\mathbf{Z}_2$-symmetry, that is, occur tangent to the space $\Sigma^\perp$. Again, we consider coordinates $\eta = x_1 + x_2$ and $\xi = x_1 - x_2$, where $\xi = (\xi_1, \xi_2)$. The normal form of the bifurcation will therefore be symmetric under the interchange of the two cells, which is equivalent to the transformation $\xi \mapsto -\xi$.

We consider the codimension two Takens-Bogdanov bifurcation that breaks the $\mathbf{Z}_2$-symmetry. The normal form of this bifurcation commutes with the symmetry $\xi \mapsto -\xi$, or equivalently, with rotation of phase space through π. The particular normal form that we discuss is

$$\begin{aligned} \xi_1' &= \xi_2 \\ \xi_2' &= p_1\xi_1 + p_2\xi_2 + a\xi_1^3 + \xi_1^2\xi_2, \end{aligned} \tag{23}$$

where p_1 and p_2 are the unfolding parameters. This particular normal form includes the coalescence of limit cycles (see [15] and section 7.3 of [8]). The two-parameter unfolding of this bifurcation is presented in Fig. 8.6.

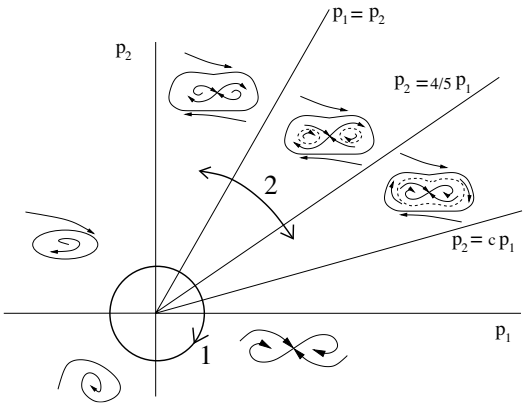

Fig. 8.6. The unfolding of the the $\mathbf{Z}_2$ symmetric Takens-Bogdanov bifurcation. Path 1 through the unfolding gives the bursting pattern shown in Fig. 8.7. After reversing the flow, path 2 results in the bursting pattern presented in Fig. 8.9. Stable limit cycles are shown by solid lines, while unstable ones are shown by dashed lines.

We assume that the center manifold in which the Takens-Bogdanov bifurcation occurs is stable. Let $\eta = x_1 + x_2 = (\eta_1, \eta_2)$ be the coordinate transverse to the center manifold. For simplicity, we assume that

$$\begin{aligned} \eta_1' &= -\lambda_1 \eta_1 \\ \eta_2' &= -\lambda_2 \eta_2 \end{aligned} \tag{24}$$

for $\lambda_1, \lambda_2 > 0$. By rewriting (23)-(24) in the x_1, x_2 coordinates we obtain a representative coupled cell system undergoing this type of bifurcation.

$$\begin{aligned} x_{11}' &= (-\lambda_1 x_{11} + x_{12} - \lambda_1 x_{21} - x_{22}) \\ x_{12}' &= (p_1 x_{11} + (p_2 - \lambda_2) x_{12} - p_1 x_{21} - (p_2 + \lambda_2) x_{22} \\ &\quad -(x_{11} - x_{21})^3 - (x_{11} - x_{21})^2 (x_{12} - x_{22})) \\ x_{21}' &= (-\lambda_1 x_{11} - x_{12} - \lambda_1 x_{21} + x_{22}) \\ x_{22}' &= (-p_1 x_{11} - (p_2 + \lambda_2) x_{12} + p_1 x_{21} + (p_2 - \lambda_2) x_{22} \\ &\quad +(x_{11} - x_{21})^3 + (x_{11} - x_{21})^2 (x_{12} - x_{22})) \end{aligned} \tag{25}$$

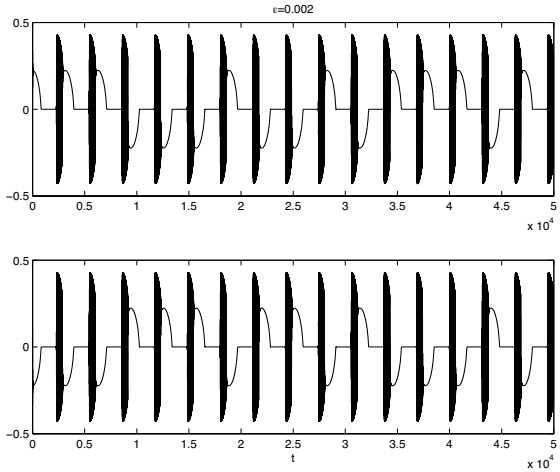

Fig. 8.7. Following path 1 in Fig. 8.6, the time series x_{11} (top) and x_{21} (bottom) are half period out of phase and attracted to the opposite limit cycles and equilibria.

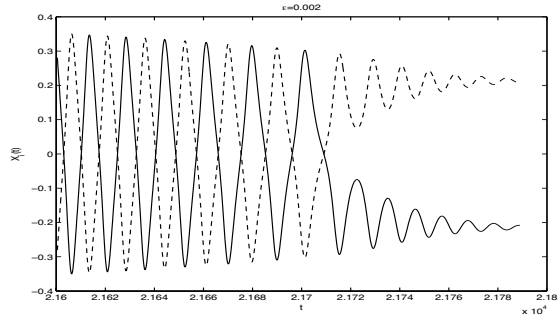

Fig. 8.8. An enlarged view of $x_{11}(t)$ and $x_{21}(t)$ together from Figure 8.7 shows the transition from antisychronous limit cycles to antisychronous equilibria.

Choosing different paths through the unfolding of this bifurcation leads to different types of bursting. Here we consider two choices leading to interesting behavior. Other paths through the unfolding can be analyzed similarly.

The first path, shown schematically as path 1 in Fig. 8.6, is given by $(p_1(\varepsilon t), p_2(\varepsilon t)) = 0.2(\cos(\varepsilon t), \sin(\varepsilon t))$. If we follow this path starting in the third quadrant, the oscillators are initially attracted to the equilibrium at the origin. This equilibrium undergoes a Hopf bifurcation at $p_2 = 0, p_1 < 0$. Since the resulting limit cycle bifurcates in the direction tangent to $\Sigma^{\perp}$, that is in the direction of $\xi = x_1 - x_2$, it leads to half period out of phase oscillations in the two cells x_1 and x_2.

This burst terminates near the line $p_2 = cp_1$ in which the stable outer limit cycle and the unstable inner limit cycle disappear in a saddle-node bifurcation. There are two stable equilibria, $(\xi^{\pm}, 0)$ with $\xi^+ = -\xi^- \neq 0$, that the system can tend to after this bifurcation. The point $(\xi^+, 0)$ corresponds to $x_{11} > x_{21}$ and $x_{12} = x_{22} = 0$, whereas the point $(\xi^-, 0)$ corresponds to $x_{11} < x_{21}$ and $x_{12} = x_{22} = 0$. Which point is chosen depends on whether the system is in the basin of attraction of the left hand or the right hand point after the attracting limit cycle disappears. Both choices are equally likely due to symmetry, and since the two basins are intertwined, one can expect different outcomes after each traversal of the path. Random switching between the two states can be seen in Figs. 8.7 and 8.8. Finally, the two points $(\xi^{\pm}, 0)$ coalesce in a subcritical pitchfork bifurcation as the slow variable re-enters the third quadrant at at $p_2 = 0, p_1 < 0$, and the entire process repeats.

In this example we observe random switching between the steady states $(\xi^{\pm}, 0)$ from one traversal of the path through the unfolding to the next. Consider the same system with time reversed (simply reverse all the arrows in Fig. 8.6). We need to compensate for the reversal of time by letting $\lambda_1 < 0$ and $\lambda_2 < 0$ in (24). In this system it is possible to observe random switching between limit cycles from burst to burst.

To illustrate this behavior we consider path 2 in Fig. 8.6, which is given by $(p_1, p_2) = 0.2(\cos(\frac{\pi}{4} + \delta \sin(\varepsilon t)), \sin(\frac{\pi}{4} + \delta \sin(\varepsilon t)))$ with $\delta = 0.1256$. The bursting resulting from this path is shown in Fig. 8.9. Note that the stable limit cycles are now denoted by dashed lines. Following the path starting in the region adjacent to the p_2 axis and proceeding clockwise, we start at one of the two stable fixed points. As in the previous examples, the two fixed points are given by $(\xi^{\pm}, 0)$. Both of these fixed points undergo a supercritical Hopf bifurcation at $p_1 = p_2$, which results in oscillations. Due to delayed

passage, these oscillations are not very prominent in Fig. 8.9, but can be observed. Approximately at $p_2 = 4/5p_1$, the two limit cycles that arose in the Hopf bifurcation coalesce in a $\mathbf{Z}_2$ symmetric homoclinic bifurcation, and give rise to a limit cycle that encompasses the origin. Again, this limit cycle corresponds to half period out of phase oscillations. The detailed analysis of the slow passage through a homoclinic bifurcation is quite involved, and we refer the reader to [5], and references therein.

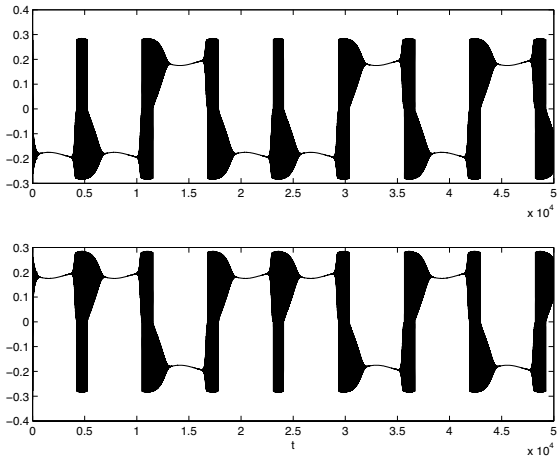

Fig. 8.9. Following path 2 (with reversal in time) in Fig. 8.6, $x_{11}(t)$ and $x_{21}(t)$, top and bottom respectively, are half period out of phase and attracted to the opposite limit cycles and equilibria.

After this bifurcation the path is traversed in the opposite direction. We first encounter the $\mathbf{Z}_2$ symmetric homoclinic bifurcation again. This bifurcation results in two limit cycles, one in the region $\xi_1 < 0$, and one in the region $\xi_1 > 0$. Which limit cycle is chosen depends on the state of the system prior to bifurcation. It is therefore expected that both limit cycles are equally likely and that it is possible to approach either. As shown in Fig. 8.9, this is indeed the case, and both types of oscillations are observed. The chosen limit cycle now disappears at a subcritical Hopf bifurcation, and the orbit settles at one of the fixed points $(\xi^-, 0)$ or $(\xi^+, 0)$ depending

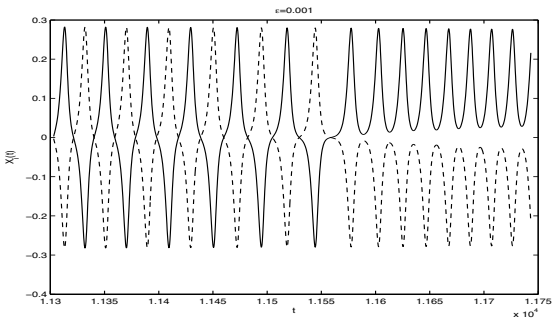

Fig. 8.10. A close view of $x_{11}(t)$ and $x_{21}(t)$ together from Fig. 8.9 shows the transition from an antisychronous limit cycle encompassing both the origin and the symmetric equilibria, to two disjoint, antisychronous limit cycles, each encompassing one of the symmetric equilibria.

on whether the system followed the left or the right limit cycle. The entire process repeats, and since, at each traversal of the path, both limit cycles arising in the $\mathbf{Z}_2$ symmetric homoclinic bifurcation are equally likely, we observe random switching between these two states from burst to burst.

8.8. Conclusion

In this chapter we have extended the ideas developed in [6] to the case of two coupled identical fast-slow systems. While these extensions are natural, the fact that we used an abstract, model independent approach may leave the reader wondering whether the phenomena we discussed can be observed in models that are used in practice.

It is natural to relate the likelihood of encountering a burster to the codimension of the bifurcation in whose unfolding it first appears. As was shown in [2, 6], the different single cell bursters most frequently encountered in applications, are, in fact, among the most likely bursters to be encountered from this viewpoint. In the present work, we have presented an overview of the phenomena that occur near low codimension bifurcations in a system of two coupled cells. In analogy to the single cell case, we can expect that these are the phenomena that are most likely to be encountered when such networks are modeled in practice.

As noted in section 8.4, a comprehensive catalog of bursting types that

can occur in the vicinity of all $\mathbf{Z}_2$ symmetric bifurcations of codimension one and two would be rather lengthy. However, an overview of the literature on these bifurcations suggests that most phenomena that can be expected have been captured in the present chapter and in [6].

Similar classifications of bursting phenomena can be made in coupled systems with symmetry and our discussion here indicates how such a classification might be pursued. However, one needs to consider low codimension equivariant bifurcations on a case by case basis. For example, in rings of cells with $\mathbf{D}_n$ symmetry, Buono *et al.* [3] show that structurally stable, asymptotically stable heteroclinic cycles can appear in Hopf / steady-state mode interactions when $n \geq 5$. Bursting phenomena when one of the stable states in the fast equations is itself a heteroclinic cycle might be quite interesting.

Acknowledgments

We thank Tasso Kaper for pointing out that bursting between in phase and out of phase periodic solutions can occur in models with $\mathbf{Z}_2$ symmetry. This work was supported in part by NSF Grant DMS-0244529.

References

[1] N. Berglund and B. Gentz, Pathwise description of dynamic pitchfork bifurcations with additive noise, *Probab. Theory Related Fields* **122**(3), 341–388, (2002).

[2] R. Bertram, M. Butte, T. Kiemel, and A. Sherman, Topological and phenomenological classification of bursting oscillations, *Bull. of Math. Bio.* **57**, 413–439, (1995).

[3] P. L. Buono, M. Golubitsky, and A. Palacios, Heteroclinic cycles in rings of coupled cells, *Physica D* **143**, 74–108, (2000).

[4] H. Crauel, P. Imkeller, and M. Steinkamp, Bifurcations of one-dimensional stochastic differential equations, In: *Stochastic dynamics (Bremen, 1997)*, Springer, New York, 27–47, (1999).

[5] D. C. Diminnie and R. Haberman, Slow passage through homoclinic orbits for the unfolding of a saddle-center bifurcation and the change in the adiabatic invariant, *Physica D* **162**(1-2), 34–52, (2002).

[6] M. Golubitsky, K. Josić, and T. J. Kaper, An unfolding theory approach to bursting in fast-slow systems, In: *Global Analysis of Dynamical Systems*, Inst. Phys., Bristol, 277–308, (2001).

[7] M. Golubitsky and D. G. Schaeffer, *Singularities and groups in bifurca-*

tion theory, Vol. I, Applied Mathematical Sciences **51**, Springer-Verlag, New York, (1985).

[8] J. Guckenheimer and P. Holmes, *Nonlinear Oscillations, Dynamical Systems, and Bifurcations of Vector Fields*, Springer-Verlag, New York, (1983).

[9] A. Harkin, T. Kaper, and A. Nadim. Coupled pulsation and translation of two gas bubbles in a liquid, *J. Fluid Mech.* **445**, 377–411, (2001).

[10] M. G. Hayes, *Geometrical Analysis of Delayed Bifurcations*, PhD thesis, Boston University, (1999).

[11] E .M. Izhikevich, Neural excitability, spiking and bursting, *Internat. J. Bifur. Chaos Appl. Sci. Engrg.* **10**(6), 1171–1266, (2000).

[12] M. Krupa and P. Szmolyan, Extending slow manifolds near transcritical and pitchfork singularities, *Nonlinearity* **14**(6), 1473–1491, (2001).

[13] J. Rinzel, Bursting oscillations in an excitable membrane model, In: *Ordinary and Partial Differential Equations (Dundee, 1984)*, Springer, Berlin, 304–316, (1985).

[14] J. Su, The phenomenon of delayed bifurcation and its analyses, In: *Multiple-Time-Scale Dynamical Systems (Minneapolis, MN, 1997)*, *IMA Vol. Math. Appl.* **122**, Springer, New York, 203–214, (2001).

[15] F. Takens, Forced oscillations and bifurcations, In: *Applications of Global Analysis, I (Sympos., Utrecht State Univ., Utrecht, 1973)*, Comm. Math. Inst. Rijksuniv. Utrecht, No. 3, 1–59. Math. Inst. Rijksuniv. Utrecht, Utrecht, (1974).

[16] D. Terman, Chaotic spikes arising from a model of bursting in excitable membranes, *SIAM J. Appl. Math.* **51**(5), 1418–1450, (1991).